Effect of Alloying Elements and Their Microsegregation on Pearlite Band Occurrence in Steels

Hyunje Sung1 and Minwoo Kang1

1Materials Research & Engineering Center, Hyundai Motor Company, Hyundaiyeonguso-ro 150, Namyang-eup, Hwaseong-si, Gyeonggi-do, 18280, Republic of Korea

Pearlite-ferrite banding (alternating bands of proeutectoid ferrite and pearlite) is commonly found in heat-treated forgings. Banding microstructure, in other words, inhomogeneous distribution of alloying elements enlarges thermal deformation variation during carburization and it is consequently detrimental to a quality of gears for automobiles. Therefore, a research was performed to examine the distribution of alloying elements and confirm its effect on the pearlite-ferrite banding using an electron probe microanalysis in alloyed steels for gears. Pearlite-ferrite banding was caused by microchemical segregation of alloying elements, especially Cr and Mn. On the other hands, banded structure was also severely caused by Nb alloying because it can reduce the prior austenite grain size smaller than the microchemical band spacing and promotes grain boundary diffusion of carbon during austenite decomposition.

Keywords: *band structure, pearlite, microsegregation, grain size, alloyed steel*

1. Introduction

Pearlite-ferrite banding is known to occur because of alloying elements having partition ratios less than 1 [1)], such as manganese, silicon, phosphorus, sulphur, aluminum and so on. They are rejected from the firstly formed delta-ferrite dendrites so that interdentritic regions have high content of them. Subsequent hot rolling or forging of the steel in the austenitic temperature region make pancaked high solute regions. During slow cooling of hot-rolled plates or hot-forgings from austenitic temperature region, interstitial carbon atoms are easier to move than substitutional atoms because of higher mobility, so regions of high carbon content will be developed in austenite originated from pancakes with high solute contents. Therefore, low and high carbon austenite regions transform to proeutectoid ferrites and pearlites, respectively [2)].

On the other hand, it is also proposed that microstructural banding is influenced by substitutional alloying elements affecting on the A_{r3} temperature [3, 4)]. During austenite decomposition, alloying elements raise or lower the A_{r3} temperature. If the solute (e.g. nickel and manganese) lowers this temperature, proeutectoid ferrite nucleates first in the solute lean regions. Conversely, if the A_{r3} temperature is raised by the solute (e.g. silicon, molybdenum), then proeutectoid ferrite forms preferentially in the solute-rich regions. In either case, carbon atoms, which can diffuse quickly, are rejected from the proeutectoid ferrite, so that austenite absorbs the carbon atoms, which eventually transform to pearlite.

Also, the effect of austenite grain size on pearlite-ferrite banding appearance was investigated [5)]. Banding tends to disappear when the austenite grain size is larger than the chemical banding wavelength. In particular, if the austenite grain size is greater than two or three times of the microchemical banding spacing, ferrite nucleates predominantly at austenite grain boundaries so that microstructural banding can be disappeared [6)].

Recently, the special steels have been developed for gears in reducers of electric vehicle and transmissions of internal combustion engine vehicle to enhance softening resistance and contact fatigue strength. But pearlite-ferrite banding can occur owing to alloying elements and it leads to unexpected and unfavorable thermal deformation during surface treatment such as carburization. Therefore, this study investigates and demonstrates how alloying elements adjusted for enhancing properties of gear steel (chromium, nickel, manganese, silicon, molybdenum, niobium and vanadium) affect on the banded microstructure.

2. Experiment

Five kinds of steel bars were prepared; their chemical compositions are listed in Table 1.

Table 1 Chemical Composition of The Steel Alloys (wt.%)

	C	Si	Mn	P	S	Cu	Cr
Alloy A	0.20	0.25	0.75	≤0.02	≤0.02	≤0.25	1.10
Alloy B	0.22	0.80	0.65	≤0.02	≤0.02	≤0.25	1.15
Alloy C	0.19	-	0.73	≤0.02	≤0.02	≤0.25	1.35
Alloy D	0.20	0.60	0.57	≤0.02	≤0.02	≤0.25	2.05
Alloy E	0.21	0.87	0.57	≤0.02	≤0.02	≤0.25	2.25
	Ni	Mo	V	Nb	O_2 (ppm)	B (ppm)	
Alloy A	-	-	-	0.025	≤25	20	
Alloy B	-	-	0.05	0.080	≤15	-	
Alloy C	-	0.60	-	0.025	≤15	-	
Alloy D	-	0.38	-	0.025	≤15	-	
Alloy E	0.35	0.30	0.65	0.025	≤15	-	

They were hot-forged at 1,200 ℃ and then air-cooled. Then, the forgings were austenitized at 930 ℃ and slowly cooled to temperatures under A_{r3} temperature, held (i.e. isothermal annealing) and finally air-cooled to room temperature.

The forgings were cut in the forging directions and microstructure was investigated using optical microscope and scanning electron microscope (SEM, FEI Quanta 450). The observed position was 3mm below the surface. Distribution and micro-segregation behavior of solutes were measured using a field emission electron probe micro-analyzer (FE-EPMA, JEOL JXA-8530F). Typical parameters were accelerating voltage of 15 kV and dwell time of 10 ms. Carbon, silicon, manganese, molybdenum, chromium, niobium and vanadium were inspected.

3. Results and discussion

All forgings showed ferrite and pearlite after isothermal annealing (Fig. 1). In particular, the Alloy B with the greatest amount of niobium content among the prepared steel in this research had pearlite-ferrite banding microstructure obviously. Solute distribution investigated by FE-EPMA revealed that carbon, manganese and chromium were enriched in pearlite band (Fig. 2), meanwhile, silicon, molybdenum, niobium and vanadium were uniformly distributed. Abrupt increase in niobium peak was detected (Fig. 2h), but it seemed that niobium-rich carbonitrides existed. Even after austenitization at 930 ℃ for 80 minutes, lots of niobium-rich carbonitrides weren't dissolve and remained in Alloy B (Fig. 3).

Before isothermal annealing, the Alloy B forging had proeutectoid ferrite, pearlite and bainite, meanwhile other steels' forgings showed bainite mostly (Fig. 4), and alloying element clustering at pearlite/bainite already occurred in the Alloy B. High niobium content in the Alloy B chromium steel could reduce austenite grain size during steel bar manufacturing and hot forging processes. This steel could have lower hardenability than chromium-molybdenum steel (Alloy C and Alloy D) and nickel-chromium-molybdenum (Alloy E). Chromium steel with boron, Alloy A, showed bainite microstructure generally because boron addition could increase hardenability, even though both Alloy B and Alloy A mainly contained chromium as alloying element.

The reason why carbon could accumulate to regions where chromium and manganese are rich is that both elements reduce carbon activity [7], so that proeutectoid ferrite grains nucleate at locations which is far from the chromium and manganese-rich regions and they grow continuously during subsequent cooling.

Due to the firstly formed ferrite grains are localized in the solutes lean regions, subsequently formed ferrites merge nearby one existed previously, then make 'slabs' of proeutectoid ferrite. Therefore, carbon atoms are driven from proeutectoid ferrite to adjacent remained austenite areas which are high in manganese and chromium, then the solutes-rich regions finally transform to pearlite.

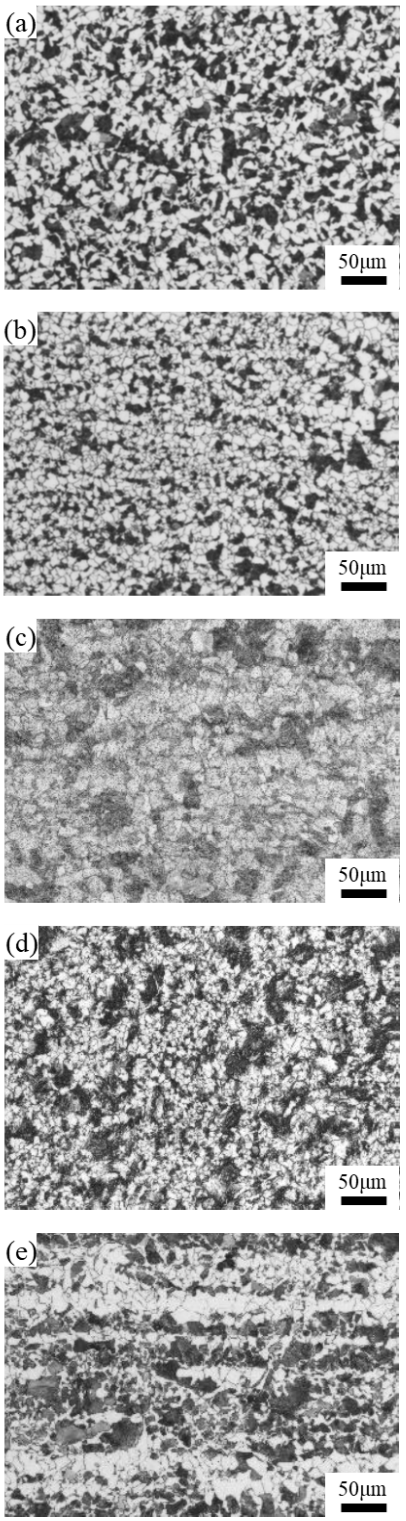

Figure 1. Optical micrographs of (a) Alloy A, (b) Alloy C, (c) Alloy D, (d) Alloy E and (e) Alloy B, respectively, observed at 3mm below the surface of forgings after the isothermal annealing.

As previously mentioned, the Alloy B remarkably showed banding phenomenon. During austenitization, the preformed niobium-rich carbonitrides exist, so growth of austenite grains are prohibited by carbonitrides, in other words, boundary pinning effect.

Refined austenite grains promote carbon atoms diffusion,

leading to severe banding formation because of faster diffusion through grain boundaries than through lattice. The explanation mentioned above is in line with previous study [5] which showed banding disappearance when austenite grain size is larger than the chemical banding wavelength.

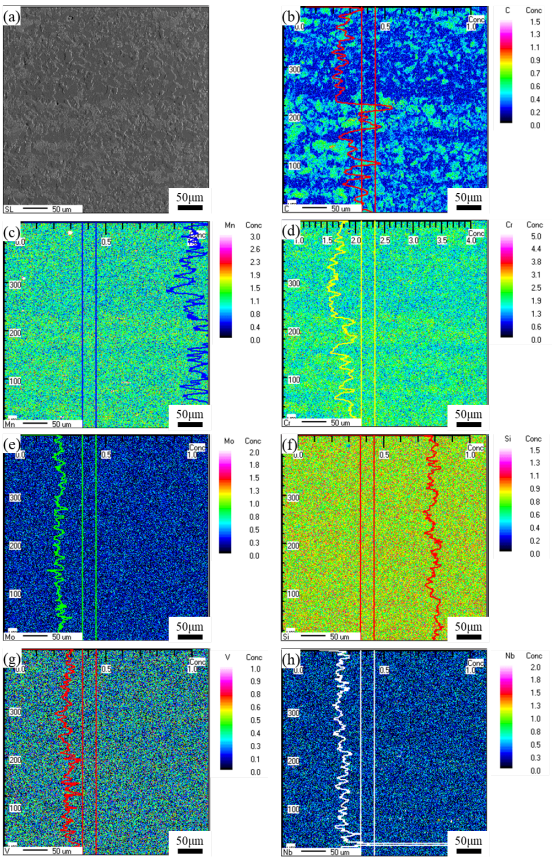

Figure 2. Alloying elements distribution maps and line scanning results of Alloy B observed at 3mm below the surface of forging after the isothermal annealing: (a) scanning electron micrograph, (b) carbon, (c) manganese, (d) chromium, (e) molybdenum, (f) silicon, (g) vanadium and (h) niobium.

In conclusion, we investigated the pearlite-ferrite banding microstructure induced by microsegregation of solutes in the special steels for gear forgings after isothermal annealing treatment. Manganese and chromium-rich regions are formed and they attract carbon atoms. On the other hand, firstly formed proeutectoid ferrite grains are localized in the solutes lean regions, ferrites merge each other and tend to make 'slabs' of proeutectoid ferrite. Remained austenite areas with high manganese and chromium content subsequently transform to pearlite. This phenomenon severely happened in the Alloy B with the greatest niobium content among the prepared steels in this study. Owing to austenite grain refinement by niobium-rich carbonitrides, carbon can easily diffuse to remained austenite area with high amounts of manganese and chromium, so that pearlite-ferrite banding can severely be formed.

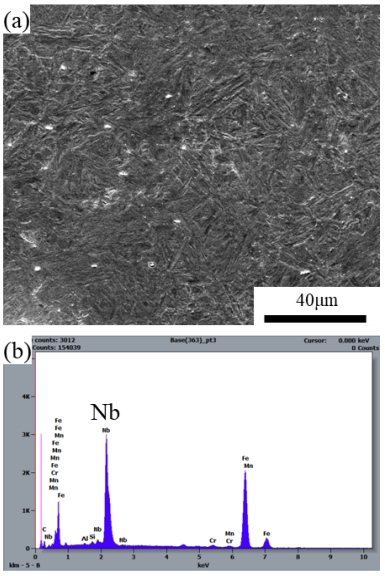

Figure 3. Niobium-rich carbonitrides in Alloy B forgings after austenitization at 930 ℃ for 80 min. and subsequent quenching to water: (a) scanning electron micrograph, (b) energy dispersive spectroscope (EDS) result of niobium-rich carbonitride.

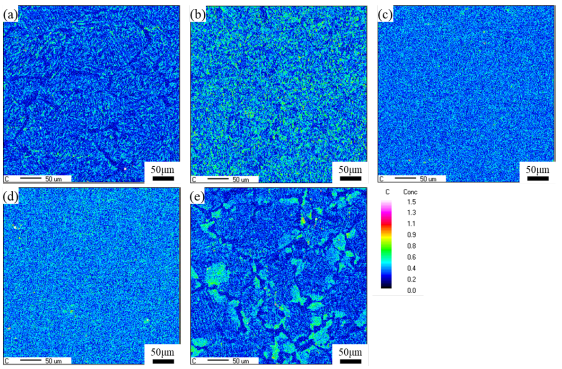

Figure 4. Carbon distribution maps observed at 3mm below the surface of forging: (a) Alloy A, (b) Alloy C, (c) Alloy D, (d) Alloy E, (e) Alloy B.

References

1) D.T. Hawkins and R. Hultgren: *Metals handbook*, (Metals Park, OH, ASM) pp. 251-338.
2) C.F. Jatczak, D.J. Girardi and E.S. Rowland: Trans. ASM. **48** (1956) 279-303.
3) P.G. Bastien: J. Iron Steel Inst., **187** (1957) 281-291
4) J.S. Kirkaldy, R.J .Brigham, H.A. Domina and R.G.Ward: Can. Metall. Q., **2** (1963) 233-241.
5) L.E. Samuels: Optical microscopy of carbon steels, (Metals Park, OH, ASM) pp. 117-167.
6) S.W. Thompson and P.R. Howell: Mater. Sci. Technol. 8 (1992) 777-784.
7) B.C.D. Cooman, J.G. Speer, I.Y. Pyshmintsev, N. Yoshinaga : *Materials Design*, pp. 151.